IEICE TRANS. ELECTRON., VOL.E106–C, NO.9 SEPTEMBER 2023

BRIEF PAPER

A Novel Displacement Sensor Based on a Frequency Delta-Sigma Modulator and its Application to a Stylus Surface Profiler

Koichi MAEZAWA[†a)], ***Senior Member***, **Umer FAROOQ**[†], ***and*** **Masayuki MORI**[†], ***Nonmembers***

SUMMARY A novel displacement sensor was proposed based on a frequency delta-sigma modulator (FDSM) employing a microwave oscillator. To demonstrate basic operation, we fabricated a stylus surface profiler using a cylindrical cavity resonator, where one end of the cavity is replaced by a thin metal diaphragm with a stylus probe tip. Good surface profile was successfully obtained with this device. A 10 nm depth trench was clearly observed together with a 10 μm trench in a single scan without gain control. This result clearly demonstrates an extremely wide dynamic range of the FDSM displacement sensors.

key words: *delta sigma modulator, frequency delta sigma modulator, microwave oscillator, displacement sensor, surface stylus profiler*

1. Introduction

A frequency delta-sigma modulator (FDSM) [1], [2] is an interesting substitute of the conventional delta-sigma modulator (DSM) [3], [4]. The FDSM is based on a voltage-controlled oscillator (VCO), which converts the input analog signal into the frequency-modulated (FM) intermediate signal. The FM signal can be easily converted to the pulse density modulated (PDM) digital signal with a simple digital circuit consisting of a register and an XOR. The FDSM is suitable for high frequency operation, because it has no feedback loop and no DAC, which restrict the operation frequency. Consequently, this technique is promising for wide band, high-resolution analog-to-digital converters (ADCs) [5]–[9].

The FDSM can be applied to sensors when the VCO is replaced by an oscillator whose oscillation frequency depends on an external physical parameter to sense. This sensor is very simple, and outputs digital signal directly. Moreover, it is robust against external noises, and eliminates noises added during signal amplification. We have recently proposed some sensors based on the FDSM concept [10]–[14]. Among these sensors, the microphone sensor based on a microwave oscillator using a cavity resonator demonstrated a very low noise power of -143 dBFS (decibel full-scale) for 96 kHz band width [11], [14]. This sensor uses a cylindrical cavity resonator for the oscillator, where one end of the resonator is replaced by a thin metal diaphragm which moves in response to sound pressure. In other words, this sensor can be regarded as a displacement sensor of the diaphragm, having a very high dynamic range. In this paper, we discuss the possibilities of such displacement sensors, and also demonstrate the application of this sensor to a stylus surface profiler.

Manuscript received December 28, 2022.
Manuscript revised March 6, 2023.
Manuscript publicized March 16, 2023.

[†]The authors are with the Faculty of Engineering, University of Toyama, Toyama-shi, 930–8555 Japan.
a) E-mail: maezawa@ieee.org

DOI: 10.1587/transele.2022ECS6013

2. The FDSM Microphone as a Displacement Sensor

Figure 1 illustrates the FDSM microphone we demonstrated in the previous paper [14] together with the block diagram of the FDSM. The variable frequency oscillator consists of a cylindrical cavity resonator and a gain block. The one end of the cavity resonator is replaced by a thin metal diaphragm, which moves in response to the sound pressure. The other end is covered by the double-sided FR-4 print circuit board (PCB), where the slots are opened on the copper GND plane to couple the microstrip lines to the cavity resonator. The size of the resonator was 25 mm diameter and 20 mm length. The resonant mode used was TE111, whose resonant frequency is approximately 10 GHz. The resonant frequency of this mode depends on the cavity length, and hence, the diaphragm position. This implementation is promising because the Q-factor of the resonator is much larger than the *LC* oscillator using a condenser microphone and an inductor [10]. This large Q-factor results in low phase noise oscillation, which is essential to obtain wide dynamic range [15].

This microphone can be regarded as a displacement sensor for the diaphragm. Here, we will discuss the advantages of the application of the FDSM microphone to dis-

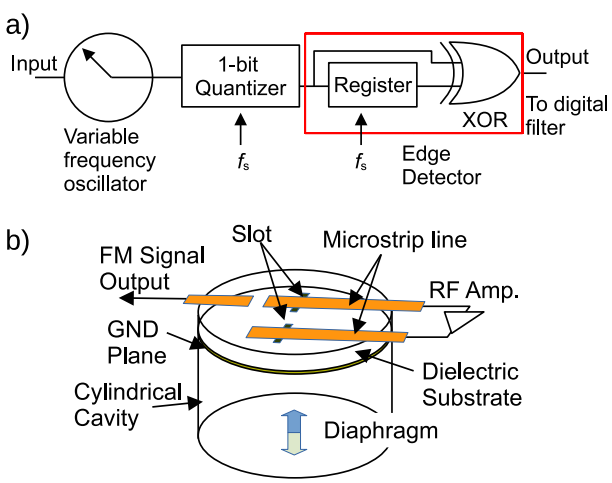

Fig. 1 The FDSM microphone fabricated in reference [14]. (a) Block diagram, (b) variable frequency oscillator sensing sound pressure.

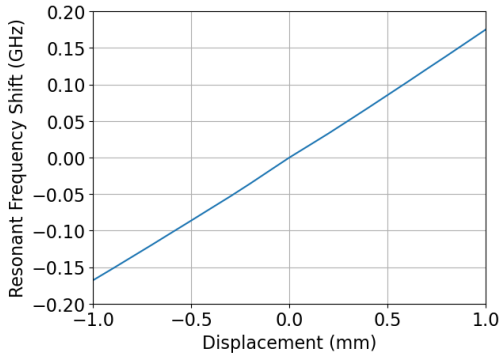

Fig. 2 Resonant frequency of the cylindrical cavity resonator calculated by EM simulation as a function of the diaphragm displacement. The diaphragm is assumed to be paraboloidal, and the displacement is measured at the center of the diaphragm.

placement sensors, especially to a surface profiler and an atomic force microscopy (AFM).

First, we will discuss the relation of the diaphragm motion to the frequency shift of the cavity resonator oscillator. For the sake of concreteness, the size of the resonator is assumed to be the same as written above throughout this paper. Figure 2 shows the resonant frequency shift as a function of the diaphragm displacement calculated by electromagnetic (EM) simulation. The diaphragm is assumed to be paraboloidal under sound pressure [16]. The figure shows that the resonant frequency shift is approximately proportional to the displacement, and the linearity is good for within ±1 mm displacement.

A significant implication in this figure is that this sensor can measure the displacement with very wide dynamic range. An extremely low total noise power of -143 dBFS was demonstrated with a sampling rate of approximately 12.6 GHz [14]. This indicates that this sensor can measure the frequency shift as small as 22 Hz. The corresponding minimum observable displacement is approximately 0.1 nm. If we assume the maximum observable displacement to be 1 mm to assure linearity, the corresponding frequency shift, 190 MHz, is still much less than maximum observable frequency shift of 3.15 GHz, which is a quarter of the sampling rate. In conclusion, ultra wide dynamic range of 0.1 nm to more than 1 mm can be obtained with this displacement sensor.

3. Application of the FDSM Microphone Sensor to a Stylus Surface Profiler and an AFM

Here, we propose and discuss application of the FDSM microphone sensor to a stylus surface profiler, and even to an atomic force microscope (AFM). Figure 3 shows the schematic of the FDSM stylus surface profiler. A stylus probe is set on the center of the diaphragm, and it is contacted to the sample, which moves with a pizoelectric stage. A most important advantage of this stylus profiler is its wide dynamic range as discussed in the previous section. It can measure the surface profile in the range from 0.1 nm to more

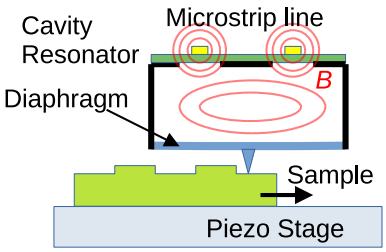

Fig. 3 A basic structure of the FDSM stylus surface profiler.

than 1 mm without changing the amplifier gain. This permits us to observe 0.1 nm class structure on a surface having 1-mm class large roughness. This technique can also be applied to AFMs when the stylus probe is replaced by an AFM tip with sophisticated diaphragm and tip design having superior mechanical properties. Important features of this type of stylus surface profilers/AFMs are follows.

First, it has a wide dynamic range with wide bandwidth. This permits us high speed scanning as well as ultra small structure measurement on a rough surface. Second, oscillating-mode, and tapping-mode measurements are also possible when applying sound waves to the diaphragm. A most important advantage of this is that the whole oscillating waveform can be precisely measured, which should include details of the atomic force. This is in contrast to the conventional AFMs, which measure the oscillating frequency shift of the cantilever. It should be noted that the oscillating frequency can be freely changed by changing the applying sound frequency, which is advantageous for measuring mechanical properties, such as elasticity, viscosity, and friction. This is difficult for the conventional AFMs that use the resonant frequency of the cantilever.

4. Prototype Device of the FDSM Stylus Surface Profiler

We have fabricated a simple prototype device of the stylus surface profiler to demonstrate the basic function. Figure 4 shows the photograph of the fabricated device. It consists of microstages, a piezoelectric stage, and a cavity resonator oscillator in a stainless frame.

Figure 5 shows the photographs of the fabricated cavity resonator oscillator. The cavity resonator was the same one used in [14]. It was fabricated from oxygen-free, high-conductivity copper to achieve a high Q-factor, which is essential for noise floor reduction. The copper block size was $45 \times 45 \times 20$ mm^3, and the cavity diameter and length were 25 mm and 20 mm, respectively. The cavity surface was polished and cleaned with a chemical cleaner to achieve a high Q-factor. The oscillator circuit on the FR-4 board is shown in Fig. 5(b), where the transmission-type oscillator topology was used to improve the phase-noise property. We used a GaAs pHEMT MMIC medium power amplifier, HMC441LP3E (Analog Devices), as the gain block of the oscillator.

For ease of fabrication, we used a microprobe pin for

the stylus probe tip. The pin was cut to a length of about 2 mm and glued to a support stand that was placed on the thin plastic plate with a diameter of 1 cm. This plastic plate was bonded to the center of the diaphragm as shown in Fig. 5(c). The diaphragm was made of commercially available 12-μm thick Al foil, the outside of which was covered with adhesive tape to suppress oscillation due to noise. The tip apex was about 10 μm in diameter.

In this experiment, no tension was intentionally applied to the diaphragm. Therefore, the force exerted by the tip on the sample can be approximately estimated from the mass of the tip support stand. The support stand was made of copper plate with a thickness of 0.1 mm. It is therefore estimated to be about 0.3 mN. This is comparable to the conventional stylus profiler. No scratch was seen on the sample surface after the measurement.

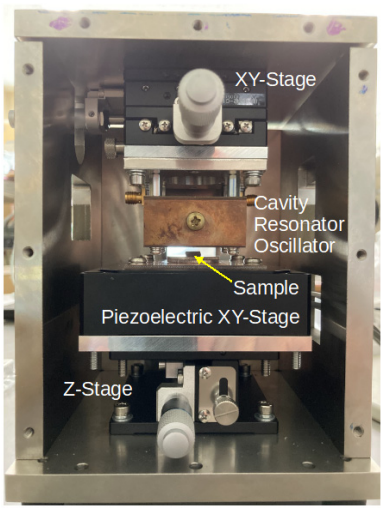

Fig. 4 Fabricated FDSM stylus surface profiler.

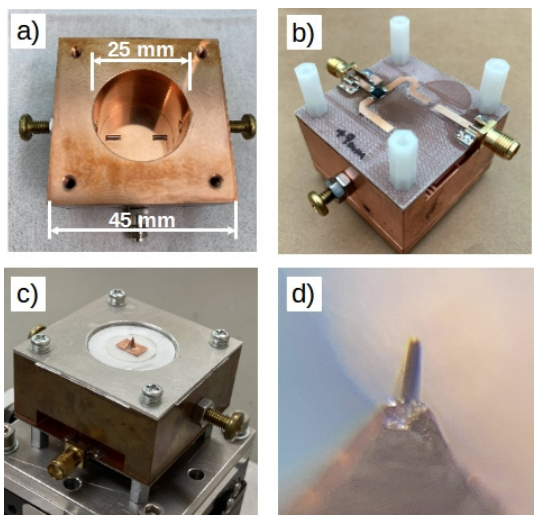

Fig. 5 Photographs of the fabricated cavity resonator oscillator. (a) Inside of the cavity resonator. The slots were shown on the bottom. (b) PCB-side of the resonator oscillator. (c) Diaphragm with a tip and support stand. (d) Apex of the tip. The apex size was approximately 10 μm.

The cavity resonator was attached on the xy-microstage for rough positioning of the measuring point, and it was set to the ceiling board downward. The piezoelectric stage was set on top of the z-microstage to adjust the sample height. The piezoelectric stage used was THK PRECISION, PS2L90-400U-S, which can control the sample's xy-position in the range of ±200 μm with a 20 nm resolution.

5. Experimental Results

We tested the basic operation of the prototype device with a GaAs sample having various depth trenches. The sample has 60-μm width trenches separated by 40-μm spaces in a line-and-space pattern. The trenches were fabricated by photolithography and wet chemical etching using sulfuric acid based etchant. The nominal depth of the trenches are 10 nm, 100 nm, 1 μm, and 10 μm, respectively. Due to the side-etching effect, the 10-μm depth trench has much wider width than that of the mask pattern. The sample was set on the PCB-based sample holder using electron wax. The sampling and digital process was done using a circuit programmed on a field programmable gate array (FPGA) board described in the reference [14]

Figure 6 shows an example of the surface profile of the sample measured by the prototype device. The depth was measured at each 4-μm step controlled by the external bias voltage applied to the piezoelectric stage. This step was smaller than the tip apex and the total number of measurement points was 100. Figure 6 was obtained from a single scan. A linear leveling procedure to compensate the sample tilting was carried out for specified two points after the

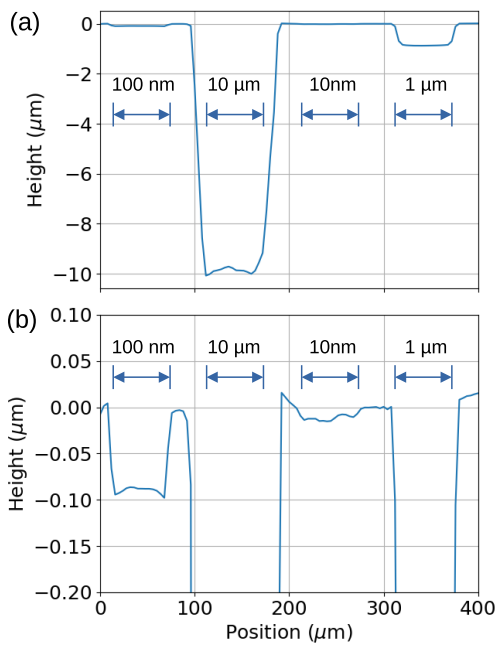

Fig. 6 An example of the measured surface profile of the GaAs line-and-space sample. The lower Fig. 6 (b) is a magnified view of the upper Fig. 6(a). The areas designated with an arrow are trenches with a nominal depth shown near the arrow.

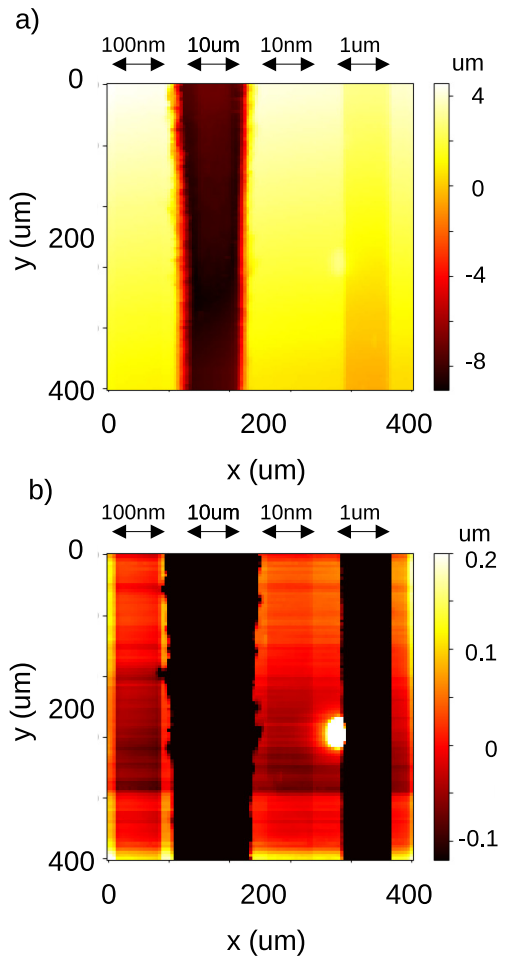

Fig. 7 An example of the 2-dimensional surface height map of the line-and-space sample. Figure 7 (a) shows an over all view, while Fig. 7 (b) shows the magnified view. The areas designated with an arrow are trenches with a nominal depth shown near the arrow.

scan. The displacement-to-frequency conversion factor was calibrated with values measured using a commercial surface profiler, and determined to be 150 kHz/μm. This factor reasonably agreed with the value determined from Fig. 2, 180 kHz/μm. The difference should be resulted from the difference in the diaphragm form due to the thin plastic plate. In Fig. 6 (a), a 1 μm depth trench is clearly seen with a large 10 μm depth trench. Moreover, a 100 nm depth trench is also visible at the left of the 10 μm trench. The Fig. 6(b) shows the magnified view of the Fig. 6(a), where the x-axis is the same as that of Fig. 6(a). Here, the 10 nm trench is also seen at the right of the 10 μm trench. It should be noted that this large dynamic range profile can be obtained in a single scan with no gain change.

Finally, we obtained surface morphology map by scanning the sample with x and y axis. An example of the results is shown in Fig. 7. Figure 7(a) shows the original map measured. Here, only 10-μm and 1-μm trenches are visible. Figure 7(b) is a magnified view of the Fig. 7(a), where the z-axis was enlarged to observe shallower structures. In this figure, the linear leveling procedure was carried out based on a plane designated by 3 points. The 100 nm trench is clearly seen at the left side of the 10 μm trench. Moreover, the 10 nm trench is also seen at the right side of the 10 μm trench. The width of the 10 μm trench is wider in Fig. 7(b), this is probably resulted from the effect of the tip apex radius. In summary, this scanned data contains information of the morphology in the range from less than 10 nm to 10 μm, which can be obtained with no gain control.

Table 1 Comparison to conventional stylus profilers

	Conventional Stylus profiler	Our proposal	
		Expected	This work
Sensor type	LVDT[*1]	FDSM	
Resolution	~ 1 nm	$\lesssim$ 0.1 nm	~ 1 nm
Max depth	~ 1 mm	$\gtrsim$ 1 mm	10 μm
Dynamic range	$\lesssim$ 90 dB[*2]	$\gtrsim$ 120 dB	~ 80 dB

[*1]Linear Variable Differential Transformer
[*2]Nominal value calculated from the range/resolution

Table 1 summarizes the results in comparison to conventional stylus surface profilers. It should be noted that the device fabricated in this experiment is a simple, prototype device to demonstrate basic operation. Nevertheless, the performance of the device is already comparable to conventional ones. Much higher performance is expected with more sophisticated diaphragm and circuit design.

6. Conclusion

A novel type of displacement sensor was proposed based on the FDSM. A cylindrical cavity resonator with a diaphragm at the one-end of the cavity was used for the variable frequency oscillator, which is a core of the FDSM. This can be applied to a stylus surface profiler and an AFM, when a probe tip is set at the diaphragm. To demonstrate basic operation, we fabricated a stylus surface profiler. Good surface profile was successfully obtained with this device. A 10 nm depth trench was measured together with a 10 μm trench in a single scan without gain control. This result clearly demonstrates the extremely wide dynamic range of the FDSM displacement sensor.

Acknowledgments

This work was supported by JSPS KAKENHI Grant Number 18H01495, and the VLSI Design and Education Center (VDEC), the University of Tokyo in collaboration with Keysight Technologies Japan, Ltd.

References

[1] M. Høvin, A. Olsen, T.S. Lande, and C. Toumazou, "Delta-sigma modulators using frequency-modulated intermediate values," IEEE J. Solid-State Circuits, vol.32, no.1, pp.13–22, Jan. 1997.
[2] A. Iwata, N. Sakimura, M. Nagata, and T. Morie, "The architecture of delta sigma analog-to-digital converters using a voltage-controlled oscillator as a multibit quantizer," IEEE Trans. Circuits Syst. II, vol.46, no.7, pp.941–945, July 1999.
[3] S.R. Norsworthy, R. Schreier, and G.C. Temes, Delta-Sigma Data Converters, IEEE Press, New York, USA, 1996.

[4] S. Pavan, R. Schreier, and G.C. Temes, Understanding Delta-Sigma Data Converters (2nd Ed.), Willey & Sons, New Jersey, 2017.
[5] M.Z. Straayer and M.H. Perrott, "A 12-bit, 10-MHz bandwidth, continuous-time ΣΔ ADC with a 5-bit, 950-MS/s VCO-based quantizer," IEEE J. Solid-State Circuits, vol.43, no.4, p.805, April 2008.
[6] M. Park and M.H. Perrott, "A VCO-based analog-to-digital converter with second-order Sigma-Delta noise shaping," IEEE Int. Symp. Circ. Sys. ISCAS, pp.3130–3133, 2009.
[7] M. Voelker, S. Pashmineh, J. Hauer, and M. Ortmanns, "Current feedback linearization applied to oscillator based ADCs," IEEE Trans. Circ. Sys. I, vol.61, no.11, pp.3066–3074, Nov. 2014.
[8] K. Lee, Y. Yoon, and N. Sun, "A scaling-friendly low-power small-area ΔΣ ADC with VCO-based integrator and intrinsic mismatch shaping capability," IEEE J. Emerg. Sel. Topic Circuits Syst., vol.5, no.4, pp.561–573, Dec. 2015.
[9] S. Li, A. Sanyal, K. Lee, Y. Yoon, X. Tang, Y. Zhong, K. Ragab, and N. Sun, "Advances in voltage-controlled-oscillator-based ΔΣ ADCs," IEICE Trans. Electron., vol.E102-C, no.7, pp.509–519, July 2019.
[10] S. Fujino, Y. Mizuno, K. Takaoka, J. Nakano, M. Mori, and K. Maezawa, "Experimental demonstration of noise shaping in the digital microphone employing frequency ΔΣ modulation," IEICE Trans. Electron. (Japanese Edition), vol.J96-C, no.12, pp.554–555, Dec. 2013.
[11] K. Maezawa, S. Fujino, T. Yamaoka, and M. Mori, "Delta-sigma modulation microphone sensors using microwave cavity resonator," Electron. Lett., vol.52, no.20, pp.1651–1652, Sept. 2016. DOI: 10.1049/el.2016.2538
[12] T. Tajika, Y. Kakutani, M. Mori, and K. Maezawa, "Experimental demonstration of strain detection using resonant tunneling delta-sigma modulation sensors," Phys. Status Solidi A, vol.214, no.3, Article No. 1600548, March 2016. DOI: 10.1002/pssa.201600548.
[13] K. Maezawa, T. Ito, and M. Mori, "Delta-sigma modulation microphone sensors employing a resonant tunneling diode with a suspended microstrip resonator," Sens. Rev., vol.40, no.5, pp.535–542, 2020. DOI: 10.1108/SR-03-2020-0044
[14] K. Maezawa, M. Mori, and H. Andoh, "Noise floor reduction in frequency delta-sigma modulation microphone sensors," Sensors, vol.21, no.10, pp.3470, May 2021. DOI:10.3390/s21103470
[15] K. Maezawa and M. Mori, "Effects of oscillator phase noise on frequency delta sigma modulators with a high oversampling ratio for sensor applications," IEICE Trans. Electon., vol.E104-C, no.9, pp.463–466, Sept. 2020. DOI: 10.1587/transele.2020ECS6026
[16] B. Liu, Transducers for Sound and Vibration - FEM Based Design, Ph.D. Thesis, Technical University of Denmark, Sec. 8, 2001.